Changes in the microstructure of compacted bentonite caused by heating and hydration

M.V. Villar[a], V. Gutiérrez-Rodrigo, R.J. Iglesias, R. Campos and L. Gutiérrez-Nebot

CIEMAT. Avd. Complutense 40, 28040 Madrid, Spain

Abstract. Two twin 40-cm long columns of compacted FEBEX bentonite were tested in Teflon cells; water was supplied through the top surface of the columns and in one of them a heater was placed at the base and set to 100°C. The purpose of these tests was to simulate the behaviour of an engineered barrier in a radioactive waste repository and investigate the effect of the thermal gradient on saturation. In particular, changes in the pore size distribution and interlayer size have been investigated in this work. The thermal gradient had a strong influence on the water intake and distribution. Water content and dry density gradients persisted in the two columns after 12 years of testing. These changes gave place to the modification of the bentonite microstructure, overall increasing the microstructural void ratio and the proportion of adsorbed, interlayer water.

1 Introduction

Geological disposal is the preferred, internationally accepted option for wastes with high levels of radioactivity or significant contents of long-lived radionuclides. The safety of repositories for radioactive waste is based on the multiple barrier concept, whereby both engineered and natural barriers between the waste and the surface act in concert to contain the wastes [1]. Deep geological repository concepts for nuclear waste disposal may include a clay barrier around the waste containers, which is the main retarding/retention component once the failure of the canister and the oxidation/dissolution of the combustible matrix are produced. Bentonites or bentonite-based materials have been usually proposed to construct this buffer around the waste container, because of their high retention capacity, low permeability and high swelling ability. The heat released by the waste will induce a thermal gradient through the bentonite barrier while groundwater will tend to flow into it. As a consequence, coupled thermal, hydraulic, mechanical and geochemical processes will take place during the transient period of the repository live. The understanding of these processes is key for the prediction of the repository evolution.

For example, it still remains unclear whether the high temperatures around the canister would hinder the full saturation of the inner part of the barrier or just delay it, but this seems to closely depend on the actual temperatures reached in the barrier and on its thickness. In most repository concepts it is expected that the temperature in the buffer be less than 100°C. At the Buffer Container Experiment performed at Lac du Bonnet (Canada), the areas of the buffer –whose thickness was 25 cm– adjacent to the heater had water contents below the initial one after 2.5 years of heating [2]. In the FEBEX in situ test, the bentonite closer to the heater had water contents below the initial ones after five years of heating (the surface temperature of the heater was of 100°C), although they were recovering after the intense initial drying (Figure 1). On the contrary, in the same period of time, the sensors located at the same distance from the gallery wall, but in an area not affected by the thermal gradient, recorded much higher relative humidity. The thickness of the bentonite barrier in this case was of 65 cm [4].

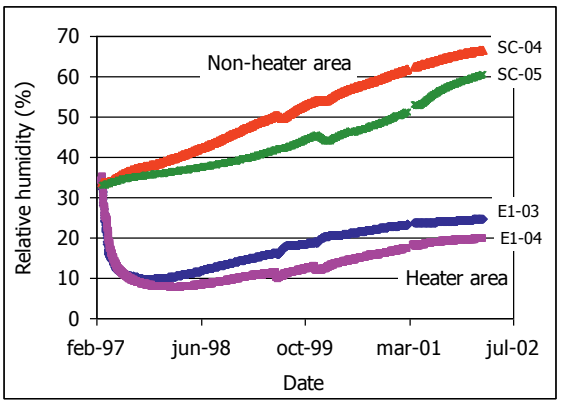

Figure 1. Evolution of the relative humidity of the bentonite recorded by two capacitive sensors located at 3.5 cm from the heater and two sensors located at approximately the same distance from the gallery wall (54 cm) in a section not affected by the heater of the FEBEX in situ test (AITEMIN data base, [3]).

[a] Corresponding author: mv.villar@ciemat.es

Conducting large-scale tests as those mentioned above is complicated and extremely costly. However, laboratory tests of different scales are very useful to identify and quantify processes in shorter periods of time. With the aim of checking the effect of the thermal gradient on water intake and redistribution, two tests were performed in cylindrical cells in which compacted bentonite was subjected to hydration through the upper surface and, in one of the cells, to heating through the base. These are called thermo-hydraulic (TH) tests and the modifications underwent by the bentonite after 12 years of testing are described below.

2 Materials and methods

2.1 Material

The FEBEX bentonite was extracted from the Cortijo de Archidona deposit (Almería, Spain) and at the factory it was disaggregated and gently ground, dried at 60°C and sieved by 5 mm, which is the maximum grain size of the material [4]. The montmorillonite content of the FEBEX bentonite is above 90 wt.%. The smectitic phases are actually made up of a smectite-illite mixed layer, with 10-15% of illite layers. Besides, the bentonite contains variable quantities of quartz, plagioclase, K-felspar, calcite and opal-CT (cristobalite-trydimite). The cation exchange capacity is 102±4 meq/100g, the main exchangeable cations being calcium (35±2 meq/100g), magnesium (31±3 meq/100g) and sodium (27±1 meq/100g).

The density of the solid particles is 2.70±0.04 g/cm^3, the hygroscopic water content 13.7±1.3 % and 67±3 percent of particles are smaller than 2 µm.

The saturated hydraulic conductivity of compacted bentonite samples is exponentially related to their dry density. For a dry density of 1.6 g/cm^3 the saturated permeability of the bentonite is about $5 \cdot 10^{-14}$ m/s at room temperature. The swelling pressure is also exponentially related to the bentonite dry density, and when the bentonite compacted at dry density 1.6 g/cm^3 is saturated with deionised water at room temperature, the swelling pressure has a value of about 6 MPa.

2.2 Thermo-hydraulic tests

The TH tests were performed in cylindrical cells whose internal diameter was 7 cm and inner length 40 cm (Figure 2). They were made of Teflon to prevent as much as possible lateral heat conduction, and externally covered with steel semi-cylindrical pieces to avoid the deformation of the cell by bentonite swelling.

Five blocks of FEBEX clay compacted with its hygroscopic water content (around 13%) at an initial nominal dry density of 1.65 g/cm^3 were stacked inside each cell. Three of the blocks had a length of 10 cm, whereas the two placed at the ends of the cells had a length of 5 cm. An average compaction pressure of 30 MPa was applied to manufacture the blocks. The bottom part of the cells was a plane stainless steel heater. In one of the tests (GT40) the clay was heated through the bottom surface at a temperature of 100ºC, which is the temperature expected on the surface of the waste container in the Spanish concept [5]. The other test (I40) was carried out at isothermal conditions (laboratory temperature). The upper closing of the cells was made by means of a stainless steel plug. Inside this plug there was a deposit in which water circulated at room temperature (20-30°C). A commercial granitic water of salinity 0.02% was injected through the upper plug of the cell at a pressure of 1.2 MPa. Its chemical composition simulated the water that saturates the barrier in a repository excavated in granitic rock.

The cells were instrumented with capacitive-type sensors placed inside the clay at three different levels separated 10 cm.

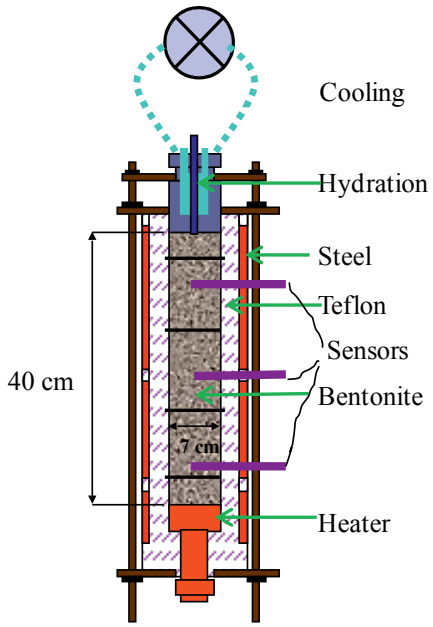

Figure 2. Schematic design of the thermo-hydraulic cells

2.3 Postmortem test

After 12 years of TH treatment the cells were dismantled and the clay columns extracted. Then the bentonite columns were sawed in 20 cylindrical sections of 2 cm in thickness used for the different analyses.

The gravimetric water content of each subsample was determined by oven drying at 110°C for 48 hours. To calculate the dry density, the volume of the specimens was determined by immersing them in a recipient containing mercury and by weighing the mercury displaced.

The pore size distribution of each subsample was determined by mercury intrusion porosimetry (MIP). Samples smaller than 3 cm^3 were lyophilised to eliminate the water in the pores. The porosimeter used was a Micromeritics AutoPore Series IV 9500, allowing the exploration of pore diameter sizes between 0.006 and 600 µm.

Other subsamples were preserved in paraffined foil and within less than an hour, the X-ray profile of a plane surface of them was registered at laboratory temperature after removing the foil and without any further treatment.

An anticatode of Cu (CuKα) radiation was used with a Philips model X'Pert-MPD diffractometer at 40 mA, 45 kV operating condition (see [6] for more details). The *d*(001) reflection or basal spacing gives the distance along the crystallographic c-axis between clay lamellae, and for a given material depends on the degree of hydration of the interlayer.

3 Results

Online results provided by the sensors during operation were presented in [7] and [8]. After 12 years of testing the relative humidity recorded by the three sensors in column I40 was about 90%. At that time, test GT40 showed a state similar to I40 in the upper 20 cm, but the sensor located at 10 cm from the heater had recorded a strong initial drying that was not recovered after 12 years of hydration. Thus, the final average relative humidity of the bentonite column I40 was higher, because the hot zones of test GT40 remained desiccated for the whole duration of the test. In this column the temperatures were practically constant during the entire test: 30±3°C at 30 cm from the heater, 36±3°C at 20 cm and 51±3°C at 10 cm (Figure 3). The latter value indicates that the thermal gradient was very steep close to the heater.

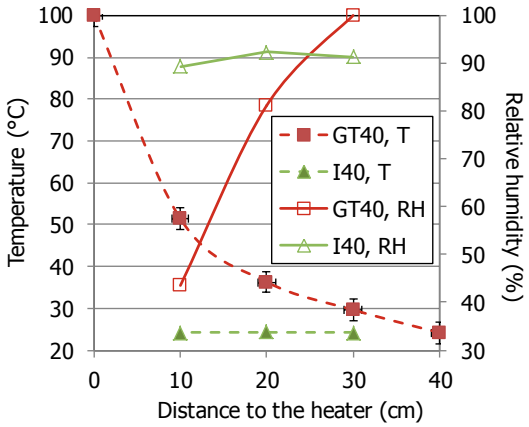

Figure 3. Steady temperatures (T) inside the bentonite during operation and final relative humidity (RH)

Upon dismantling it was observed that the five blocks that formed column I40 were sealed, whereas only the three upper ones were sealed in column GT40. It was also checked that the o-rings at the base of the latter had seriously degraded, which let evaporation take place through the bottom part of the cell for an unknown period of time during operation.

3.1 Final physical state

The gravimetric water content measured at the end of the tests ranged from 35% at the top in both columns to 23% at the bottom in the isothermal test (test I40) and to 3% near the heater in the column subjected to thermal gradient (test GT40). The dry densities had changed according to the swelling caused by hydration, being lower towards the hydration surface (Figure 4). The high swelling pressure developed by the bentonite upon saturation deformed the Teflon cells in spite of the external steel reinforcement, which allowed an overall increase of the columns' volume, causing a decrease of the bentonite dry density from 1.65 g/cm^3 to 1.46 g/cm^3 in test I40 and to 1.55 g/cm^3 in test GT40. The final average water content was higher in test I40 (27.7% *vs.* 20.4%) but the water content and dry density gradients were steeper in test GT40. The final degree of saturation was about 100% in the 5 and 10 cm closest to the hydration surface in column GT40 and I40, respectively and lower in the rest of the columns [9].

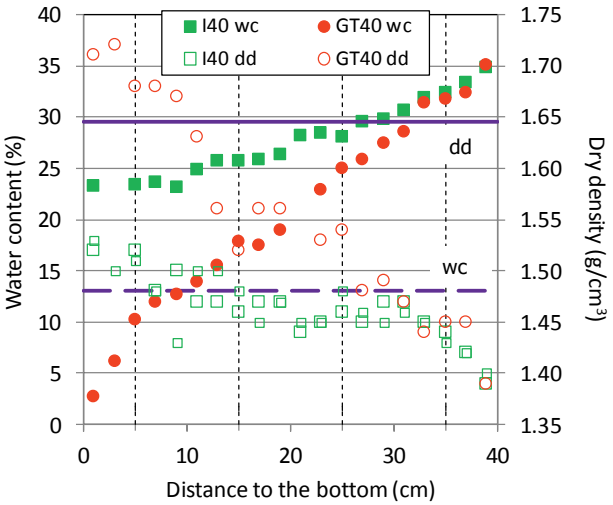

Figure 4. Final water content (wc) and dry density (dd) along the columns (the horizontal thick lines indicate the initial values and the vertical dotted lines the separation between blocks inside the columns)

3.2 Pore size distribution

The pore size distribution of samples taken along the columns was analysed by mercury intrusion porosimetry. Due to the limitations of the method, only part of the macropores (pores of sizes between $6{\cdot}10^5$ and 50 nm) and part of the mesopores (pores between 50 and 6 nm) were explored. It is not expected to find pores larger than $6{\cdot}10^5$ nm in compacted clay materials, but the number of pores smaller than 6 nm can be very relevant. To overcome this undervaluation of porosity, an estimation of the percentage of pores not intruded by mercury can be made by comparing the actual void ratio of the samples (computed from their dry density and density of solid particles) and the apparent void ratio calculated from mercury intrusion. Thus, the pore size distribution curves obtained by MIP were corrected to take into account the percentage of pores not intruded. For the sake of clarity only a few curves of each test are shown in Figure 5 and Figure 6. Both Figures include the pore size distribution curve for a sample compacted to 1.6 g/cm^3 with hygroscopic water content, which would represent the initial conditions of the bentonite blocks.

Two pore families appeared systematically in all the samples, one in the size range of macropores and another one in the size range of mesopores. This is the usual pore size distribution pattern obtained by MIP in compacted

FEBEX bentonite, irrespective of the water content or dry density. The percentage of pores intruded was on average of 50%, which is slightly below the percentage of pores intruded in the original material. Additionally, more than 60% of the pores of all the samples had a diameter smaller than 50 nm after testing, which meant a slight increase in this pore size range with respect to the original material. Both observations point to an increase in the number of the smallest pores after testing.

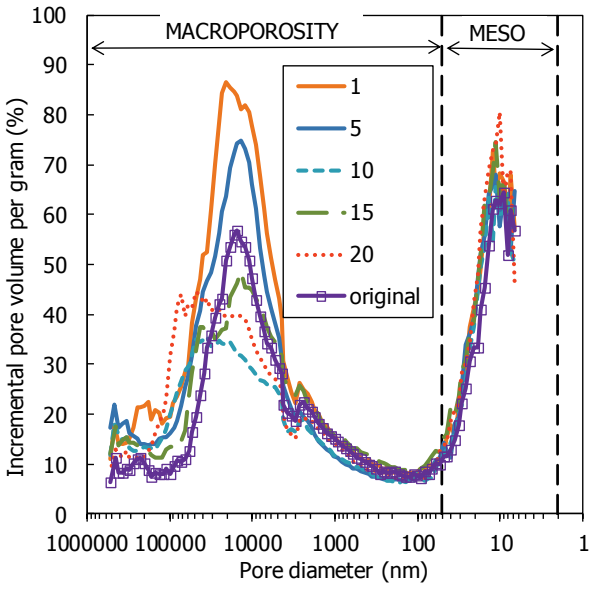

Figure 5. Pore size distribution of samples from test I40 (1: 39 cm from bottom, 5: 35 cm, 10: 21 cm, 15: 11 cm, 20: 1 cm) and of a sample compacted at 1.6 g/cm^3 with *w*=14% (original)

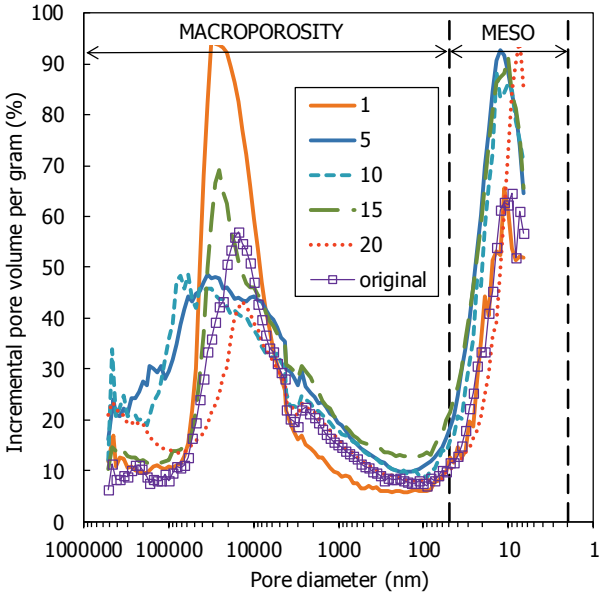

Figure 6. Pore size distribution of samples from test GT40 (1: 39 cm from bottom, 5: 35 cm, 10: 23 cm, 15: 11 cm, 20: 1 cm) and of a sample compacted at 1.6 g/cm^3 with *w*=14% (original)

Assuming that the percentage of pores not intruded by mercury corresponded entirely to pores of size smaller than 6 nm (the limit of the equipment) and assimilating this percentage to the micropore size (which is not totally right, since micropores are those smaller than 2 nm), an estimation of the percentage of micropores could be inferred from the percentage of pores non-intruded. The percentage of each pore size could thus be recalculated. Following the terminology proposed in some constitutive models [10], the pores of sizes <50 nm (i.e. micro and mesopores) would constitute the microstructure, where physico-chemical and other phenomena take place at particle level, whereas larger pores would represent the capillary-controlled macrostructure. Taking into account the measured void ratio of the samples and the recalculated percentage of each pore size, the micro and macrostructure void ratios were computed and are plotted in Figure 7. Hydration brought an increase in void ratio with respect to the original values, due to the swelling allowed by the cell deformation (see section 3.1). In column I40 there was an overall significant increase in microstructural void ratio with respect to the original material, whereas the macro void ratio increased only in the most hydrated part of the column. The macro void ratio evolution was similar in test GT40, as was the increase in microstructural void ratio in the most hydrated upper part of the column. However, at approximately 15 cm from the hydration surface, the microstructural porosity started to decrease sharply towards the heater. In fact, the final micro void ratio in the 10 cm closest to the heater in test GT40 was below the initial one. This was the part of the column where the dry density increased above the initial value due to water evaporation and shrinkage (Figure 4).

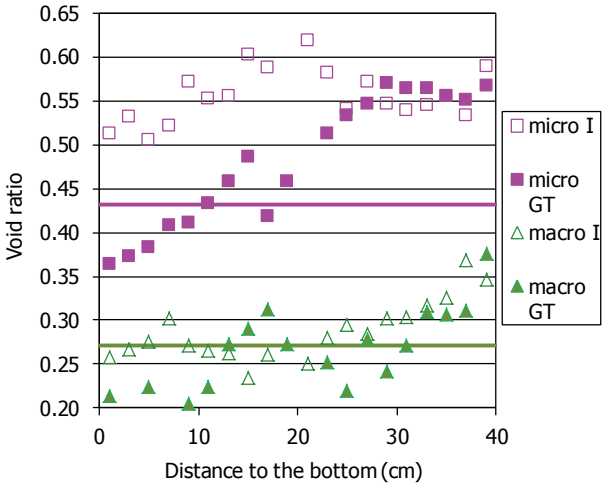

Figure 7. Microstructural and macrostructural void ratio along the two columns at the end of the tests (the horizontal thick lines indicate the initial values)

3.3 Interlayer distance

The basal spacing of the smectite was determined by X-ray diffraction in samples preserved to keep the same density and water content as upon dismantling. This value gives a measure of the interlayer distance between

smectite particles, a minimum value of about 1 nm corresponding to a collapsed interlayer with no water in it. It is considered that smectites display basal spacings of about 1.25, 1.55 and 1.85 nm for the homogeneous 1, 2 and 3 water layers hydration states, respectively.

The values measured were similar all along column I40 with an average value of 1.64 nm, whereas in test GT40 changed from 1.83 to 1.26 nm from the top to the bottom of the heater. This means that the interlayer of the bentonite would have between 2- and 3-layer hydrates in all the samples of test I40 and from almost 3-layer hydrates near the hydration surface to 1-layer hydrate close to the heater in test GT40 (Figure 8). Under hygroscopic water content, which was the condition of the bentonite at the beginning of the tests, the basal spacing of the FEBEX bentonite is about 1.48 nm. Hence, the interlayer distance increased during the tests all along column I40 and in the upper 25 cm of column GT40, i.e. where the water content was higher than the initial one (Figure 4).

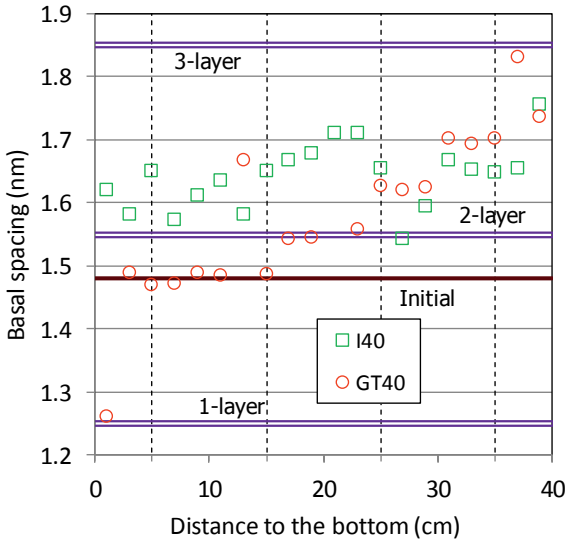

Figure 8. Basal spacings measured by XRD in unaltered samples at the end of the TH tests and in the initial sample (horizontal line). The horizontal bands indicate the range of spacings corresponding to the different hydration states

In fact, the basal spacing can be related to the water content almost lineally, although with a large dispersion for the higher water contents, as can be seen in Figure 9, where the results have been plotted again expressed in Å (1 nm = 10 Å). The basal spacings measured in compacted FEBEX bentonite saturated with water in the liquid or in the vapour phase and under free or confined volume conditions (taken from [6] are also plotted in the same figure). The dispersion of these data was attributed to the different dry density and hydration time of the samples, which was in all cases much shorter than the duration of tests I40 and GT40. It can be observed that the values for the two TH tests follow the same trend, which shows that the interlayer water retention capacity did not decrease over time, on the contrary, the values obtained after 12 years of TH treatment tended to be higher for the same water content.

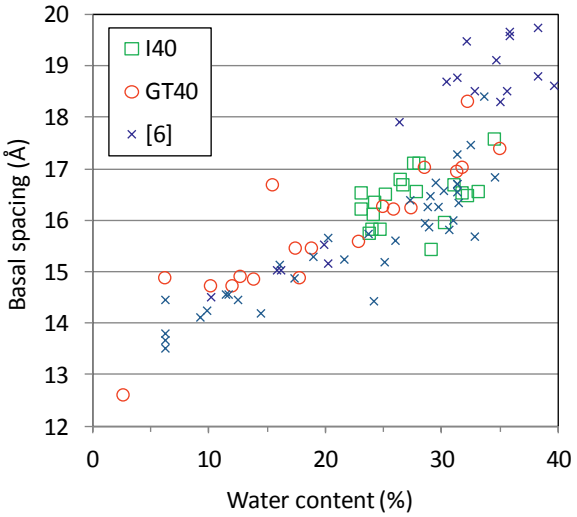

Figure 9. Basal spacing of FEBEX samples compacted to different dry densities and saturated in different ways [6] and those measured at the end of tests I40 and GT40

4 Concluding remarks

Two thermo-hydraulic tests in cells performed with compacted FEBEX bentonite run for almost 12 years. In one of them the column of bentonite was hydrated under thermal gradient (GT40) and in the other one at isothermal conditions (I40). The tests provided online information about the temperature and relative humidity inside the bentonite [7, 8]. Finally they were dismantled and the physical state of the bentonite was analysed.

There were water content and dry density gradients along both bentonite columns, sharper for cell GT40. The water content had increased with respect to the initial one all along column I40, whereas in the 15 cm closest to the heater in test GT40 the water content was lower than the initial and the dry density higher, due to evaporation and shrinkage. Despite the fact that the macrostructural void ratio increased with respect to the original value in the most hydrated part of the two columns, the final micro/macro void ratio relation was higher than the initial all along the two columns. However, the microstructural void ratio decreased towards the heater in column GT40.

The interlayer distances measured were correlated with the water content, increasing with it as expected. However, for a given water content, the basal spacings measured tended to be higher than those in samples that had the same water contents for much shorter periods of time (reported in previous investigations). This could be a consequence of the water redistribution over time, which brought an increase in the number of layer hydrates with time probably correlated with the increase in microporosity observed in the MIP tests. This implies that the maturation of the barrier would lead to a decrease in free water availability, since most water would eventually enter the interlayer porosity.

The fact that the Teflon cells could deform during the tests due to the high swelling of the bentonite upon saturation, giving place to an overall decrease of the columns density, and that evaporation took place through the bottom of column GT40 are experimental artefacts

that must be taken into account when extrapolating these results to the real barrier case, in which none of these processes will take place. As well, the temperatures in column GT40 were lower than those expected in a real repository, due to the different geometry and heat dissipation allowed by the experimental setup [8].

These tests have highlighted the influence of the thermal gradient on the hydration kinetics, the persistence of the water content and dry density gradients and the slowness of the saturation process. As well, the changes in water content and density occurred gave place to the modification of the bentonite microstructure, on the whole increasing the microstructural void ratio and the proportion of adsorbed, interlayer water.

References

1. N. Chapman, C. McCombie, *Waste Management Series, 3* (Elsevier, Amsterdam, 2003)
2. D. Dixon, N. Chandler, J. Graham, M.N. Gray, Can. Geotech. J. **39**, 503-518 (2002)
3. M.V. Villar, *Informes Técnicos CIEMAT 1044* (CIEMAT, Madrid, 2004)
4. ENRESA, *Publicación Técnica ENRESA 05-0/2006* (ENRESA, Madrid, 2006)
5. ENRESA, *Publicación Técnica ENRESA 11/95* (ENRESA, Madrid, 1995)
6. M.V. Villar, R. Gómez-Espina, L. Gutiérrez-Nebot, Applied Clay Science **65-66**, 95-105 (2012a)
7. M.V. Villar, R. Gómez-Espina, *Informes Técnicos CIEMAT 1178* (CIEMAT, Madrid, 2009)
8. M.V. Villar, P.L. Martín, I. Bárcena, J.L. García-Siñeriz, R. Gómez-Espina, A. Lloret, Eng. Geology **149-150**, 57-69 (2012b)
9. M.V. Villar, R. Gómez-Espina, P.L. Martín, F.J. Romero, R.J. Iglesias, *XXIII Reunión SEA 2014, Libro de resúmenes*, 79-80 (2014)
10. A. Gens, E. Alonso, Canadian Geotech. J. **29**, 1013-1032 (1992)